

# Fourier's law from a chain of coupled planar harmonic oscillators under energy-conserving noise

Gabriel T. Landi<sup>1,2</sup> and Mário J. de Oliveira<sup>2</sup>

<sup>1</sup>*Centro de Ciências Naturais e Humanas, Universidade Federal do ABC, Santo André, São Paulo 09210-170, Brazil*

<sup>2</sup>*Instituto de Física, Universidade de São Paulo, Caixa Postal 66318, 05314-970 São Paulo, Brazil*

(Received 25 September 2013; published 6 February 2014)

We study the transport of heat along a chain of particles interacting through a harmonic potential and subject to heat reservoirs at its ends. Each particle has two degrees of freedom and is subject to a stochastic noise that produces infinitesimal changes in the velocity while keeping the kinetic energy unchanged. This is modeled by means of a Langevin equation with multiplicative noise. We show that the introduction of this energy-conserving stochastic noise leads to Fourier's law. By means of an approximate solution that becomes exact in the thermodynamic limit, we also show that the heat conductivity  $\kappa$  behaves as  $\kappa = aL/(b + \lambda L)$  for large values of the intensity  $\lambda$  of the energy-conserving noise and large chain sizes  $L$ . Hence, we conclude that in the thermodynamic limit the heat conductivity is finite and given by  $\kappa = a/\lambda$ .

DOI: [10.1103/PhysRevE.89.022105](https://doi.org/10.1103/PhysRevE.89.022105)

PACS number(s): 05.70.Ln, 05.10.Gg, 05.60.-k

## I. INTRODUCTION

Fourier's law of heat conduction states that the heat flux  $J$  is proportional to the gradient of temperature, that is,  $J = -\kappa \nabla T$ , where  $\kappa$  is the heat conductivity. Since this law is understood as a *macroscopic* description of a nonequilibrium phenomenon, it seems natural to address the problem of deriving Fourier's law from a *microscopic* model. However, this task has proved to be incredibly challenging. Indeed, despite being over 200 years old, to this day, no definitive microscopic model for this law has yet been agreed on. The first attempt was made by Rieder *et al.* [1], who considered a linear chain of particles connected by harmonic forces, with the first and last particles coupled to Langevin reservoirs at different temperatures. Their calculations showed that this model yields a ballistic (instead of a diffusive) heat flow. If we write  $J = \kappa \Delta T/L$ , where  $L$  is the size of the system, then ballistic flow means that  $J$  is constant so that, in the thermodynamic limit ( $L \rightarrow \infty$ ),  $\kappa$  diverges. Hence, the finiteness of  $\kappa$  in the thermodynamic limit serves as a criterion for the validity of Fourier's law.

The ballistic nature of the harmonic chain incites the idea that a new ingredient is necessary to yield the correct diffusive behavior. Indeed, several variations of the harmonic chain have been studied in recent decades. These include the use of anharmonic interactions [2–12], systems with disorder [13,14], self-consistent reservoirs [15–18], and many others [19–32]. Many of these attempts lead to anomalous diffusion, for which  $\kappa$  is also infinite. Some, however, do lead to Fourier's law. An important example is the self-consistent reservoir model introduced by Bolsterli *et al.* [15]. In this model all particles (and not just the first and the last) are connected to heat reservoirs whose temperatures are chosen such that, in the steady state, there is no exchange of energy between the reservoirs and the inner particles of the chain (i.e., all except the first and the last).

An essential requirement in the construction of a microscopic model leading to Fourier's law is that heat should be exchanged only through the end points of the chain: no energy should enter or leave the system through the inner particles. Notice that the self-consistent model, strictly speaking, does not meet this requirement. A recent approach that fulfils this

requirement and leads to Fourier's law (in the harmonic chain) is based on the introduction of an energy-conserving noise that flips the sign of the velocity with some given rate [33,34]. This noise models the interaction of the chain with additional degrees of freedom in the medium. In the present paper we are concerned with a new type of energy-conserving noise, which closely resembles elastic collisions in a solid and, as we will show, leads to Fourier's law. This is accomplished by the introduction of infinitesimal random changes of the velocity, modeled by a Langevin equation with multiplicative noise devised so that it conserves the kinetic energy.

The main features of our study are as follows. First, it indicates that the relevant property required to induce Fourier's law is the energy-conserving nature of the noise and not its fine details or the mechanism with which it is implemented. Second, when compared to the aforementioned velocity-flipping model, this new noise has a more natural interpretation as elastic collisions of the atoms in a crystal with other microscopic degrees of freedom. Third, by modeling this noise by means of a Langevin equation with multiplicative noise, it becomes possible to recast the problem in terms of a system of linear equations for the position-velocity covariances. Solving numerically this linear problem is not only faster than solving numerically the Langevin equation but also gives a much deeper insight into the problem. From the covariances we obtain an approximate expression for the heat conductivity for large chain sizes and large intensities of the energy-conserving noise. This expression, as will be shown, becomes exact in the thermodynamic limit. Moreover, we also present exact expressions in the opposite situation of small system sizes. Finally, the nonequilibrium steady state (NESS) is shown to be Gaussian, so that it is entirely defined by the covariances.

We will consider the usual linear chain with harmonic potentials and with the first and last particles connected to Langevin heat baths at different temperatures. However, we allow each particle to have two degrees of freedom. This simple variation enables us to introduce *infinitesimal* random rotations of the velocities of each particle. To see how this type of noise is introduced let us consider for the time being only a single particle with unit mass, free to move in the  $xy$  plane, and let  $v$  and  $u$  denote the velocity components of this particle in the

$x$  and  $y$  directions, respectively. Now, consider the following Langevin equations with multiplicative noise [35]:

$$\frac{dv}{dt} = -\lambda v - \sqrt{2\lambda} u \zeta, \quad (1)$$

$$\frac{du}{dt} = -\lambda u + \sqrt{2\lambda} v \zeta, \quad (2)$$

where  $\zeta(t)$  is a standard Gaussian white noise and  $\lambda$  represents the rate (or the intensity) of the noise; notice that the noise  $\zeta(t)$  is the same in both equations, but their signs are distinct. One can easily show that the magnitude of the velocity  $(v^2 + u^2)^{1/2}$  is invariant. From this result, it follows that the kinetic energy is conserved so that these Langevin equations appropriately describe random elastic collisions of the particle with the medium. They make up the key point of our model. For completeness, we also write the Fokker-Planck equation associated with the Langevin equations (1) and (2),

$$\frac{\partial P}{\partial t} = \lambda \left\{ \frac{\partial(vP)}{\partial v} + \frac{\partial(uP)}{\partial u} + u^2 \frac{\partial^2 P}{\partial v^2} + v^2 \frac{\partial^2 P}{\partial u^2} - 2 \frac{\partial^2(uvP)}{\partial u \partial v} \right\}. \quad (3)$$

It shows that the intensity of the collisions  $\lambda$  may be taken as the inverse of a characteristic time constant.

As will be shown below, the inclusion of this new type of random elastic collisions in the harmonic chain correctly leads to Fourier's law. Moreover, in the thermodynamic limit, we find that  $\lambda$  acts as a relevant parameter. That is, no matter how small it is, as long as  $\lambda \neq 0$ , the system will obey the correct diffusive behavior. When  $\lambda = 0$ , we recover the ballistic model of Rieder *et al.* [1].

When  $\lambda$  and the system size  $L$  are large enough, it is possible to obtain an exact result for the heat conductivity, which, as we will show, behaves as

$$\kappa = \frac{aL}{b + \lambda L}, \quad (4)$$

where  $a$  and  $b$  are independent of  $\lambda$  and  $L$ , even though they depend on other parameters of the model. Therefore, in the thermodynamic limit the heat conductivity is finite and given by  $\kappa = a/\lambda$ .

## II. MODEL

We now describe the model studied in this paper. Consider a chain of  $L$  particles, each with two degrees of freedom. Their positions are denoted by  $x_i$  and  $y_i$ , and their velocities are denoted by  $v_i = dx_i/dt$  and  $u_i = dy_i/dt$ , with  $i = 1, \dots, L$ . The equations of motions, assuming unit mass, are

$$\frac{dv_i}{dt} = f_i - \lambda v_i - \sqrt{2\lambda} u_i \zeta_i - \gamma_i v_i + \sqrt{2\gamma_i T_i} \xi_i^x, \quad (5)$$

$$\frac{du_i}{dt} = g_i - \lambda u_i + \sqrt{2\lambda} v_i \zeta_i - \gamma_i u_i + \sqrt{2\gamma_i T_i} \xi_i^y, \quad (6)$$

where  $f_i$  and  $g_i$  are the  $x$  and  $y$  components of the force acting on the  $i$ th particle and  $\zeta_i(t)$ ,  $\xi_i^x(t)$ , and  $\xi_i^y(t)$  are independent standard Gaussian white noises. The parameters  $\gamma_i$  are zero except when  $i = 1$  and  $i = L$ , in which case  $\gamma_1 = \gamma_L = \gamma$ .

They describe the contact of the system with two reservoirs at temperatures  $T_1 = T_A$  and  $T_L = T_B$ . The Boltzmann constant is set to unity. We note that the most relevant parameter is  $\lambda$ , the intensity of the random elastic collisions.

The set of Langevin equations (5) and (6) may also be interpreted as describing two coupled one-dimensional chains of particles. One is described by the variables  $x_i$  and  $v_i$ , and the other is described by the variables  $y_i$  and  $u_i$ . The energy-conserving noise is interpreted as a stochastic noise that changes the velocity of two particles belonging to distinct chains in such a way that their combined kinetic energies remain constant. This interpretation is very natural and can be extended, for instance, to several one-dimensional chains.

The Fokker-Planck equation associated with the Langevin equations (5) and (6), which describes the time evolution of the probability distribution, is given by

$$\frac{\partial P}{\partial t} = - \sum_i \left( \frac{\partial v_i P}{\partial x_i} + \frac{\partial u_i P}{\partial y_i} + \frac{\partial \hat{f}_i P}{\partial v_i} + \frac{\partial \hat{g}_i P}{\partial u_i} \right) + \sum_i \left( \frac{\partial^2 D_i^x P}{\partial v_i^2} + \frac{\partial^2 D_i^y P}{\partial u_i^2} - 2\lambda \frac{\partial^2 v_i u_i P}{\partial v_i \partial u_i} \right), \quad (7)$$

where

$$\hat{f}_i = f_i - (\gamma_i + \lambda)v_i, \quad \hat{g}_i = g_i - (\gamma_i + \lambda)u_i, \quad (8)$$

$$D_i^x = \gamma_i T_i + \lambda u_i^2, \quad D_i^y = \gamma_i T_i + \lambda v_i^2. \quad (9)$$

The forces are assumed to be conservative; that is, they are the gradient of a potential energy  $U$ ,  $f_i = -\partial U/\partial x_i$  and  $g_i = -\partial U/\partial y_i$ . When the system is uncoupled from the heat reservoirs, the total energy

$$E = \sum_{i=1}^L \frac{m}{2} (v_i^2 + u_i^2) + U \quad (10)$$

is a constant of motion. Thus, in this case the system evolves in isolation and, due to the random elastic collisions, is ergodic; that is, it reaches an equilibrium given by the Gibbs microcanonical distribution. When the system is coupled to the heat baths, the change in the total energy is entirely due to the exchange of energy with the heat bath. If the temperatures of the heat baths are the same, the equilibrium distribution is the Gibbs canonical distribution.

In this paper we focus on harmonic potentials, which yield closed equations for the covariances, as we shall see below. The harmonic potential  $U$  that we use has the general form

$$U = \frac{1}{2} \sum_{ij} A_{ij} x_i x_j + \frac{1}{2} \sum_{ij} B_{ij} y_i y_j + \sum_{ij} C_{ij} x_i y_j, \quad (11)$$

where  $A_{ij}$ ,  $B_{ij}$ , and  $C_{ij}$  are understood as the elements of  $L \times L$  matrices  $A$ ,  $B$ , and  $C$ .

We have used several types of harmonic potentials, and all lead to Fourier's law. For definiteness, we shall consider here three specific forms of  $U$ , all involving nearest-neighbor interactions.

(I) The first type of potential is symmetric and uncoupled in  $x$  and  $y$ . It is given by

$$U_1 = \frac{k}{2} \sum_{i=0}^L [(x_i - x_{i+1})^2 + (y_i - y_{i+1})^2], \quad (12)$$

where  $x_0 = x_{L+1} = y_0 = y_{L+1} = 0$ . When compared to (11), we see that  $A$  is the tridiagonal matrix

$$A = k \begin{pmatrix} 2 & -1 & 0 & 0 & 0 & \dots & 0 & 0 \\ -1 & 2 & -1 & 0 & 0 & \dots & 0 & 0 \\ 0 & -1 & 2 & -1 & 0 & \dots & 0 & 0 \\ 0 & 0 & -1 & 2 & -1 & \dots & 0 & 0 \\ \vdots & \vdots & \vdots & \vdots & \vdots & \ddots & \vdots & \vdots \\ 0 & 0 & 0 & 0 & 0 & -1 & 2 & -1 \\ 0 & 0 & 0 & 0 & 0 & 0 & -1 & 2 \end{pmatrix}, \quad (13)$$

whereas  $B = A$  and  $C = 0$ . This choice of potential treats  $x$  and  $y$  on equal footing and does not couple them. Hence, they are connected only through the energy-conserving noise. In the stationary state the heat flux is determined by the position-velocity covariance, which, in this case, is given by

$$J = 2k \langle x_i v_{i+1} \rangle. \quad (14)$$

(II) The second type of potential is still symmetric in  $x$  and  $y$  but couples both directions. It is given by

$$U_2 = \frac{k}{2} \sum_{i=0}^L [(x_i - x_{i+1})^2 + (y_i - y_{i+1})^2 + 2\alpha(x_i - x_{i+1})(y_i - y_{i+1})], \quad (15)$$

where, again,  $x_0 = x_{L+1} = y_0 = y_{L+1} = 0$ . The parameter  $\alpha$  is chosen within the interval  $0 \leq \alpha \leq 1$  in order to guarantee mechanical stability. Referring to Eq. (11), we have  $B = A$  and  $C = 2\alpha A$ , where  $A$  is the tridiagonal matrix given by (13). In the stationary state the heat flux is given by

$$J = 2k[\langle x_i v_{i+1} \rangle + \alpha \langle x_i u_{i+1} \rangle]. \quad (16)$$

(III) The third type of potential is asymmetric and pinned in  $y$ . It is given by

$$U_3 = \frac{k}{2} \sum_{i=0}^L (x_i - x_{i+1})^2 + \frac{k'}{2} \sum_{i=1}^L y_i^2. \quad (17)$$

Now we have  $x_0 = x_{L+1} = 0$ . In this case  $C = 0$ ,  $A$  is the tridiagonal matrix given by (13), and  $B = (k'/2)I$ , where  $I$  is the  $L \times L$  identity matrix. In the stationary state the heat flux is given by

$$J = k \langle x_i v_{i+1} \rangle. \quad (18)$$

Finally, in all cases the heat conductivity is computed from

$$\kappa = |JL/\Delta T|. \quad (19)$$

### III. COVARIANCES

#### A. General harmonic potentials

The linearity of the harmonic forces and the type of energy-conserving noise we use here allow us to find closed equations

for the covariances, which can be solved by standard (numerically exact) procedures. It is useful to define  $x = (x_1, \dots, x_L)$ ,  $v = (v_1, \dots, v_L)$ ,  $y = (y_1, \dots, y_L)$ , and  $u = (u_1, \dots, u_L)$ , all interpreted as column vectors. The  $L \times L$  covariance matrices are defined by the expectation of the outer products:

$$X_1 = \langle xx^\dagger \rangle, \quad X_2 = \langle yy^\dagger \rangle, \quad X_3 = \langle xy^\dagger \rangle, \quad (20)$$

$$Y_1 = \langle vv^\dagger \rangle, \quad Y_2 = \langle uu^\dagger \rangle, \quad Y_3 = \langle vu^\dagger \rangle, \quad (21)$$

$$Z_1 = \langle xv^\dagger \rangle, \quad Z_2 = \langle yu^\dagger \rangle, \quad (22)$$

$$Z_3 = \langle xu^\dagger \rangle, \quad Z_4 = \langle yv^\dagger \rangle. \quad (23)$$

The full  $4L \times 4L$  covariance matrix is

$$\Theta = \begin{pmatrix} \Theta_1 & \Theta_3 \\ \Theta_3^\dagger & \Theta_2 \end{pmatrix} = \begin{pmatrix} X_1 & Z_1 & X_3 & Z_3 \\ Z_1^\dagger & Y_1 & Z_4^\dagger & Y_3 \\ X_3^\dagger & Z_4 & X_2 & Z_2 \\ Z_3^\dagger & Y_3^\dagger & Z_2^\dagger & Y_2 \end{pmatrix}. \quad (24)$$

The evolution equations for the covariances are obtained from the Fokker-Planck equation as follows. Consider, for instance, the covariance  $\langle x_i x_j \rangle$ , which is an entry of  $X_1$ . Multiply both sides of Eq. (7) by  $x_i x_j$  and take the average. The left-hand side gives the time derivative  $d\langle x_i x_j \rangle/dt$ . Performing the integrals in the right-hand side by parts, as many times as necessary, we get the desired time evolution equation. Repeating this procedure for all covariances, we reach the equation

$$\frac{d}{dt} \Theta = -(\Phi \Theta + \Theta \Phi^\dagger) + \Upsilon - \lambda \Psi, \quad (25)$$

where the  $4L \times 4L$  matrix  $\Phi$  is

$$\Phi = \begin{pmatrix} \Phi_1 & \Phi_3 \\ \Phi_3 & \Phi_2 \end{pmatrix} = \begin{pmatrix} 0 & -I & 0 & 0 \\ A & \Gamma & C & 0 \\ 0 & 0 & 0 & -I \\ C & 0 & B & \Gamma \end{pmatrix}, \quad (26)$$

where  $I$  is the  $L \times L$  identity matrix and  $\Gamma$  is the diagonal matrix with elements  $\Gamma_{11} = \Gamma_{LL} = \gamma$ , with all other entries being zero. The other  $4L \times 4L$  matrices appearing in Eq. (25) are as follows:

$$\Upsilon = \begin{pmatrix} \Upsilon_1 & 0 \\ 0 & \Upsilon_1 \end{pmatrix} = \begin{pmatrix} 0 & 0 & 0 & 0 \\ 0 & D & 0 & 0 \\ 0 & 0 & 0 & 0 \\ 0 & 0 & 0 & D \end{pmatrix}, \quad (27)$$

where  $D$  is a  $L \times L$  diagonal matrix with elements  $D_{11} = 2\gamma T_A$  and  $D_{LL} = 2\gamma T_B$ , again with all other entries being zero. Moreover,

$$\Psi = \begin{pmatrix} \Psi_1 & \Psi_3 \\ \Psi_3^\dagger & \Psi_2 \end{pmatrix} = \begin{pmatrix} 0 & Z_1 & 0 & Z_3 \\ Z_1^\dagger & 2(Y_1 - \bar{Y}_2) & Z_4^\dagger & 2(Y_3 + \bar{Y}_3) \\ 0 & Z_4 & 0 & Z_2 \\ Z_3^\dagger & 2(Y_3^\dagger + \bar{Y}_3) & Z_2^\dagger & 2(Y_2 - \bar{Y}_1) \end{pmatrix}, \quad (28)$$

where  $\bar{Y}_1$ ,  $\bar{Y}_2$ , and  $\bar{Y}_3$  are  $L \times L$  diagonal matrices composed of the diagonal elements of  $Y_1$ ,  $Y_2$ , and  $Y_3$ , respectively.

In the stationary state, which interests us here, Eq. (25) becomes

$$(\Phi\Theta + \Theta\Phi^\dagger) + \lambda\Psi = \Upsilon, \quad (29)$$

which can be written in an equivalent form, in terms of  $2L \times 2L$  matrices,

$$(\Phi_1\Theta_1 + \Theta_1\Phi_1^\dagger) + (\Phi_3\Theta_3^\dagger + \Theta_3\Phi_3^\dagger) + \lambda\Psi_1 = \Upsilon_1, \quad (30)$$

$$(\Phi_2\Theta_2 + \Theta_2\Phi_2^\dagger) + (\Phi_3\Theta_3 + \Theta_3^\dagger\Phi_3^\dagger) + \lambda\Psi_2 = \Upsilon_1, \quad (31)$$

$$(\Phi_1\Theta_3 + \Theta_3\Phi_2^\dagger) + (\Phi_3\Theta_2 + \Theta_1\Phi_3^\dagger) + \lambda\Psi_3 = 0. \quad (32)$$

Note that Eqs. (30) and (31) are coupled through the matrices  $\Psi_1$  and  $\Psi_2$  since in  $\Psi_1$  there is a term containing  $\bar{Y}_2$  and vice versa [cf. Eq. (28)].

Let us consider particular cases of these equations. When the potential is symmetric under the transformations  $x_i \rightleftharpoons y_i$  and  $v_i \rightleftharpoons u_i$ , like that given by (12) and (15), then  $B = A$ , so that  $\Phi_2 = \Phi_1$ . Moreover, the Fokker-Planck equation will also be invariant under  $x_i \rightleftharpoons y_i$  and  $v_i \rightleftharpoons u_i$  and so will the covariances, leading to the symmetric solution  $\Theta_2 = \Theta_1$ ,  $\Psi_2 = \Psi_1$ , and  $\Theta_3^\dagger = \Theta_3$ . Equations (30)–(32) are then reduced to

$$(\Phi_1\Theta_1 + \Theta_1\Phi_1^\dagger) + (\Phi_3\Theta_3 + \Theta_3\Phi_3) + \lambda\Psi_1 = \Upsilon_1, \quad (33)$$

$$(\Phi_1\Theta_3 + \Theta_3\Phi_1^\dagger) + (\Phi_3\Theta_1 + \Theta_1\Phi_3^\dagger) + \lambda\Psi_3 = 0. \quad (34)$$

If, furthermore, the variables  $x$  and  $y$  are not coupled, for instance, when  $U$  is given by (12), then  $C = 0$ , so that  $\Phi_3 = 0$ . In this case Eqs. (33) and (34) become two independent equations for  $\Theta_1$  and  $\Theta_3$ ,

$$(\Phi_1\Theta_1 + \Theta_1\Phi_1^\dagger) + \lambda\Psi_1 = \Upsilon_1, \quad (35)$$

$$(\Phi_1\Theta_3 + \Theta_3\Phi_1^\dagger) + \lambda\Psi_3 = 0. \quad (36)$$

From this last equation, it follows that the interchain covariances vanish,  $\Theta_3 = 0$  and  $\Psi_3 = 0$ , and we are left only with Eq. (35) for  $\Theta_1$ .

Let us consider now an unsymmetrical potential like the one given by (17) for which  $C = 0$ , so that  $\Phi_3 = 0$ ,  $A \neq 0$ , and  $B \neq 0$ . Moreover,  $B$  is a diagonal matrix. In this case we get

$$(\Phi_1\Theta_1 + \Theta_1\Phi_1^\dagger) + \lambda\Psi_1 = \Upsilon_1, \quad (37)$$

$$(\Phi_2\Theta_2 + \Theta_2\Phi_2^\dagger) + \lambda\Psi_2 = \Upsilon_1, \quad (38)$$

$$(\Phi_1\Theta_3 + \Theta_3\Phi_2^\dagger) + \lambda\Psi_3 = 0. \quad (39)$$

The equation for  $\Theta_3$  again gives  $\Theta_3 = 0$ . Equations (37) and (38) are coupled through the diagonal covariances  $\bar{Y}_1$  and  $\bar{Y}_2$  that appear in  $\Psi_2$  and  $\Psi_1$ , respectively.

## B. Numerical results

Before continuing with the analytical development of our model, we briefly stop to present a numerical analysis. Most of our discussion will focus on the symmetric potential  $U_1$  in Eq. (12). The other choices of potential do not change any of the important conclusions we shall obtain. In what

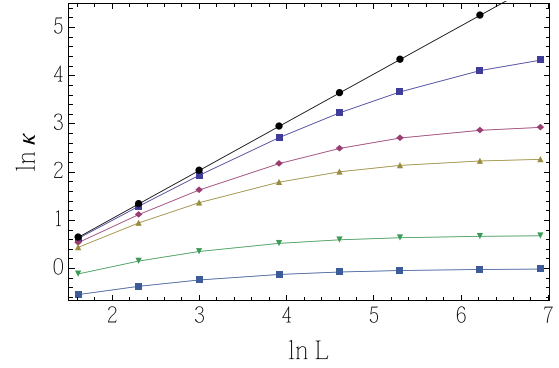


FIG. 1. (Color online) Thermal conductivity  $\kappa$  as a function of the system size  $L$  for different values of  $\lambda$ , the intensity of the elastic collisions: from top to bottom,  $\lambda = 0, 0.01, 0.05, 0.1, 0.5$ , and  $1$ . The calculations are for the potential  $U_1$  in Eq. (12) with fixed  $k = 1$ ,  $\gamma = 1$ ,  $T_A = 1$ , and  $T_B = 2$ .

follows we fix  $k = 1$ ,  $\gamma = 1$ ,  $T_A = 1$ , and  $T_B = 2$ . The free parameters are  $\lambda$  (the intensity of the elastic collisions) and  $L$  (the size of the system). For this choice of potential we may obtain the steady-state covariances by solving Eq. (35) numerically, which is simpler than the general equation (29) valid for arbitrary harmonic potentials. We then compute the heat flux from Eq. (14) and finally the heat conductivity from the relation  $\kappa = |JL/\Delta T|$ .

In Fig. 1 we show results for  $\kappa$  as a function of  $L$ , for both  $\lambda = 0$  and  $\lambda \neq 0$  (several values). When  $\lambda = 0$ , we see clearly that  $\kappa \propto L$ , which means that we recover the ballistic results of Ref. [1]. In fact, these results can even be compared with their exact solution. This is so because, due to our choice of potential, when  $\lambda = 0$ , the  $x$  and  $y$  directions are independent, so that the heat conductivity is simply twice the original result for the one-dimensional chain. When  $\lambda \neq 0$ , we find that as  $L$  increases,  $\kappa$  tends to a finite value. The rapidity with which this asymptotic limit is reached increases with increasing  $\lambda$ . Regardless, we may conjecture that irrespective of how small  $\lambda$  is, in the thermodynamic limit ( $L \rightarrow \infty$ ) this asymptotic value is always reached. This seems reasonable from the results of Fig. 1 and will also be corroborated by further arguments to be given below. Figure 2 illustrates the dependence of  $\kappa$  on  $\lambda$  for different values of  $L$ . Note the broad range covered by  $\lambda$ , from  $10^{-4}$  to  $10^2$ . This is a consequence of the efficiency of the numerical method just discussed. Figure 2 shows that, when  $L \rightarrow \infty$ ,  $\kappa \propto 1/\lambda$ .

In summary, from Figs. 1 and 2 we find the following scaling behavior: when  $L \rightarrow \infty$ ,  $\kappa \propto 1/\lambda$ , and when  $\lambda = 0$ ,  $\kappa \propto L$ . We therefore assume the following scaling law [33]:

$$\kappa = \frac{a'L}{b' + \lambda L}, \quad (40)$$

valid for small values of  $\lambda$  and large values of  $L$ . A fitting of this finite-size scaling is presented in Fig. 3, where the collapse of the data points can be clearly observed. The finite-size scaling formula (40) clearly shows that  $\lambda$  is a relevant parameter: as long as  $\lambda \neq 0$ , in the thermodynamic limit we always obtain a finite value of  $\kappa$ .

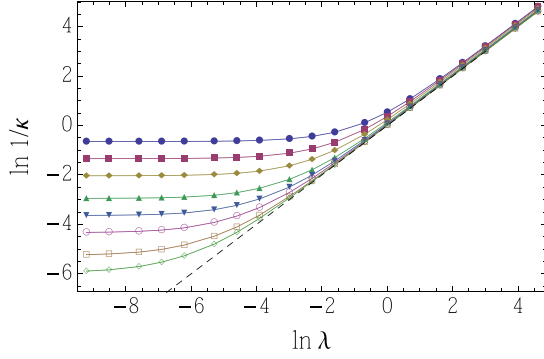


FIG. 2. (Color online) Plot of  $1/\kappa$  vs  $\lambda$  for different values of  $L$ : from top to bottom  $L = 5, 10, 20, 50, 100, 200, 500$ , and  $1000$ . The calculations are for the potential  $U_1$  in Eq. (12) with the same parameters as in Fig. 1.

For completeness, in Fig. 4 we also present the scaling behavior obtained for the other potentials,  $U_2$  and  $U_3$ , defined in Eqs. (15) and (17), respectively. The parameters  $a'$  and  $b'$  in Eq. (40) were fitted to the data. As can be seen, a very similar behavior is obtained, which corroborates our claim that the choice of potential is unimportant in obtaining Fourier's law.

#### IV. ANALYTICAL RESULTS

##### A. Symmetric and uncoupled potential

We now return to Eq. (35) for the covariances under the potential  $U_1$  and show how it can be simplified. Written explicitly, Eq. (35) gives  $Z^\dagger = -Z$  and

$$(AZ - ZA) + (\Gamma Y + Y\Gamma) + 2\lambda(Y - \bar{Y}) = D, \quad (41)$$

$$(AX - XA) - (Z\Gamma + \Gamma Z) = 2\lambda Z, \quad (42)$$

$$2Y - (XA + AX) - (Z\Gamma - \Gamma Z) = 0, \quad (43)$$

where we have dropped the indices in  $X_1, Y_1$ , and  $Z_1$ .

Here we reach a remarkable result. These equations are exactly the same equations for the covariances in the velocity-flipping model, Eq. (7) of Ref. [34], which may therefore

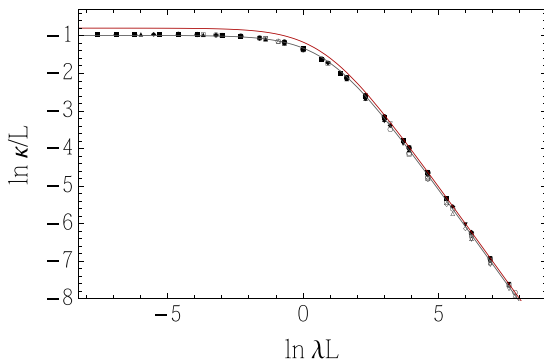


FIG. 3. (Color online) Finite-size scaling of  $\kappa/L$  vs  $\lambda L$  for the potential  $U_1$ , Eq. (12), with parameters  $k = 1, \gamma = 1, T_A = 1$ , and  $T_B = 2$ . The bottom solid line is a fitting to the data points from Eq. (40) with parameters  $a'$  and  $b'$ . The top solid line represents the solution (55).

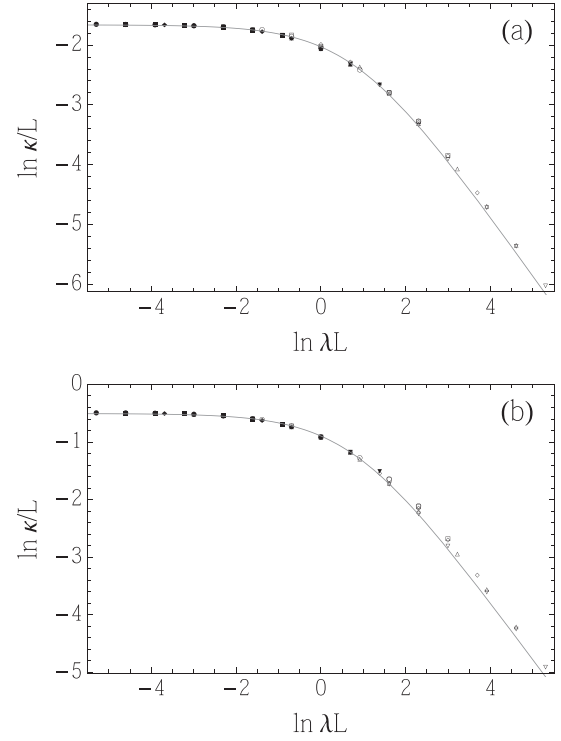


FIG. 4. Finite-size scaling of  $\kappa/L$  vs  $\lambda L$  for the potentials (a)  $U_2$  (with  $\alpha = 0.5$ ) and (b)  $U_3$  (with  $k' = 1$ ) in Eqs. (15) and (17). The solid line represents a fit from Eq. (40) with fit parameters  $a'$  and  $b'$ . The other parameters are  $k = 1, \gamma = 1, T_A = 1$ , and  $T_B = 2$ .

be interpreted as a particular case of our velocity-rotation model. It is important to note, however, that the fact that the equations for the covariances coincide does not imply that both models are identical. For instance, the equations governing the evolution of the probability distribution of both models are entirely different, which can be seen by noting that in the present model it is described by a standard Fokker-Planck equation, whereas in the velocity-flipping model the conserving noise is modeled by a master-equation-type term [34]. The facts that both models give the same equations for the covariances and hence that both lead to Fourier's law mean that the rather sharp nature of the velocity-flipping model [33,34] is not the relevant ingredient to induce Fourier's law. What is, in fact relevant, is the energy-conserving nature of the noise.

We begin our analysis by subtracting the equilibrium solution  $X^e, Y^e$ , and  $Z^e$  from the covariance matrices  $X, Y$ , and  $Z$ . Recall that the nonvanishing elements of  $D$  are  $D_{11} = 2\gamma T_A$  and  $D_{LL} = 2\gamma T_B$ . The equilibrium covariances  $X^e$  and  $Y^e$  are solutions of

$$(\Gamma Y^e + Y^e \Gamma) = D^0, \quad (44)$$

$$(A X^e - X^e A) = 0, \quad (45)$$

$$2Y^e - (X^e A + A X^e) = 0, \quad (46)$$

where  $D^0$  is the  $L \times L$  diagonal matrix with nonvanishing elements  $D_{11}^0 = D_{LL}^0 = 2\gamma T$  and  $T = (T_A + T_B)/2$ . Notice that the velocity-velocity covariance matrix  $Y^e$  is diagonal and the position-velocity covariances vanish,  $Z^e = 0$ .

Next, we define the dimensionless matrices  $X^*$ ,  $Y^*$ , and  $Z^*$  by

$$X = X^e + \frac{X^* \Delta T}{\gamma^2}, \quad (47)$$

$$Y = Y^e + Y^* \Delta T, \quad (48)$$

$$Z = Z^e + \frac{Z^* \Delta T}{\lambda}, \quad (49)$$

where  $\Delta T = T_B - T_A$ . The equations for  $X^*$ ,  $Y^*$ , and  $Z^*$  are obtained by subtracting the equilibrium solution (44)–(46) from (41)–(43). Let us work with dimensionless quantities  $A'$  and  $\Gamma'$  defined by  $A = kA'$  and  $\Gamma = \gamma\Gamma'$ . We also define  $d$  as the diagonal matrix with elements  $d_{11} = 1$  and  $d_{LL} = -1$ . As a result we obtain the set of equations

$$\varepsilon \nu (A' Z^* - Z^* A') + (\Gamma' Y^* + Y^* \Gamma') + \frac{2}{\varepsilon} (Y^* - \bar{Y}^*) = d, \quad (50)$$

$$\nu (A' X^* - X^* A') - \varepsilon (Z^* \Gamma' + \Gamma' Z^*) = 2Z^*, \quad (51)$$

$$\nu (A' X^* + X^* A') + \varepsilon (Z^* \Gamma' - \Gamma' Z^*) = 2Y^*, \quad (52)$$

where  $\nu = k/\gamma^2$  and  $\varepsilon = \gamma/\lambda$  are now the only two free dimensionless parameters. As before,  $\bar{Y}^*$  is the diagonal matrix formed by the diagonal elements of  $Y^*$ . These equations do not involve either  $T_A$  or  $T_B$ , which shows that  $X^*$ ,  $Y^*$ , and  $Z^*$  do not depend on temperature. Now, from Eq. (14) and from the definition of the covariance  $Z$  we see that the heat flux is  $J = 2kZ_{n,n+1} = 2kZ_{n,n+1}^* \Delta T/\lambda$ , from which we may write the following relation for the heat conductivity:

$$\kappa = \frac{2kL Z_{n,n+1}^*}{\lambda}. \quad (53)$$

Since  $Z^*$  does not depend on temperature, we conclude that the heat conductivity does not depend on temperature. This result is valid for any harmonic potential and is a direct consequence of the linearity of the equations for the covariances [1].

It is worth mentioning an important property concerning the position-velocity covariances. If we consider the diagonal elements of the left- and right-hand sides of Eq. (50), we get the following result:

$$Z_{12}^* = Z_{23}^* = \dots = Z_{L-1,L}^*, \quad (54)$$

which reflects the invariance of the heat flux along the chain and shows that  $\kappa$ , given by (53), does not depend on  $n$ , as it should. It also reflects the conservation of energy inside the chain. Incidentally, in the original harmonic chain [1], which is obtained from our model by setting  $\lambda = 0$ , the matrix  $Z$  is a Toeplitz matrix, and Eq. (54) is thus fulfilled. When  $\lambda \neq 0$ , even though the first diagonal is still constant, as in Eq. (54), the same is not true of the others.

### B. Large $\lambda$ expansion

As will be shown in this section, the heat conductivity in the limit of large  $\lambda$  and large  $L$  is described by

$$\kappa = \frac{kL}{\frac{k}{\gamma} + c\gamma + \lambda L}, \quad (55)$$

where  $c$  is found numerically to be  $c = 1.20938909(5)$ . We call attention to the fact that, in the thermodynamic limit,  $\kappa = k/\lambda$  and the heat conductivity is thus independent of the coupling constant  $\gamma$ . Formula (55) is depicted by the top solid line in Fig. 3. As can be seen, it agrees quite well with the simulations when  $\lambda L$  is large. The agreement, as is expected, becomes worse when  $\lambda L$  is small.

The purpose of this section is to derive formula (55) for the heat conductivity, valid for large  $L$  and large  $\lambda$ . Exact expressions for the heat conductivity  $\kappa$ , Eq. (53), can be obtained by exactly solving Eqs. (50)–(52) for small chains. As shown in Appendix A, the results always have the same form of a ratio of polynomials in  $\lambda$ , in which the numerator is a polynomial of one order less than the denominator. The results obtained for small chains, from  $L = 2$  up to  $L = 14$ , show that when  $\lambda$  is large, the heat conductivity has the form

$$\kappa = \frac{kL S_L}{\frac{k}{\gamma} S_L + \gamma C_L + \lambda L}, \quad (56)$$

where  $S_L$  and  $C_L$  are rational numbers that depend on  $L$ . In Appendix A we show the exact values of these numbers for  $L = 2$  up to  $L = 5$ . Next, we shall show that this formula is, in fact, valid for any  $L$  and that  $S_L$  and  $C_L$  approach finite values,  $S_L \rightarrow 1$  and  $C_L \rightarrow c$ , when  $L \rightarrow \infty$ , thus recovering Eq. (55).

We start by considering the solution of Eqs. (50)–(52) for large  $\lambda$  or, which is equivalent, small  $\varepsilon$ . We shall therefore assume that  $X^*$ ,  $Y^*$ , and  $Z^*$  can be written as a series expansion in  $\varepsilon$  of the form

$$X^* = X^0 + \varepsilon X^I + \varepsilon^2 X^{II} + \dots, \quad (57)$$

$$Y^* = Y^0 + \varepsilon Y^I + \varepsilon^2 Y^{II} + \dots, \quad (58)$$

$$Z^* = Z^0 + \varepsilon Z^I + \varepsilon^2 Z^{II} + \dots. \quad (59)$$

Since  $\kappa$  is given by Eq. (53), we may also write

$$\kappa = \kappa^I \varepsilon + \kappa^{II} \varepsilon^2 + \dots, \quad (60)$$

where

$$\kappa^I = \frac{2kL}{\gamma} Z_{n,n+1}^0, \quad \kappa^{II} = \frac{2kL}{\gamma} Z_{n,n+1}^I. \quad (61)$$

Thus, our goal now is to find the functions  $Z_{n,n+1}^0$  and  $Z_{n,n+1}^I$ .

Let us write down the ensuing equations for each order of  $\varepsilon$  that stem from Eqs. (50)–(52). In order  $1/\varepsilon$  the only contribution is found in Eq. (50) and gives

$$Y^0 = \bar{Y}^0, \quad (62)$$

i.e.,  $Y^0$  is diagonal. To order zero in  $\varepsilon$  we find the following system of equations:

$$(\Gamma' Y^0 + Y^0 \Gamma') + 2(Y^I - \bar{Y}^I) = d, \quad (63)$$

$$\nu (A' X^0 - X^0 A') = 2Z^0, \quad (64)$$

$$\nu (A' X^0 + X^0 A') = 2Y^0. \quad (65)$$

From Eq. (63) we may reach two conclusions. First, by looking at the diagonal entries we find that

$$Y_{11}^0 = -Y_{LL}^0 = 1/2. \quad (66)$$

Second, since the right-hand side is diagonal, we find that

$$Y^I = \bar{Y}^I, \quad (67)$$

i.e.,  $Y^I$  is also diagonal ( $Y^{II}$  will no longer be diagonal, so  $Y^*$  itself is *not* diagonal).

We may now use Eqs. (64) and (65) to eliminate  $X^0$ . The result is

$$A'Z^0 + Z^0A' = A'Y^0 - Y^0A'. \quad (68)$$

This matrix equation should be solved subject to the constraint (54) and the boundary condition (66). It is equivalent to  $L(L-1)/2$  linear equations. Taking into account Eq. (54), there are  $(L^2 - 3L + 4)/2$  unknown entries for  $Z^0$ . Similarly, taking into account Eq. (66), there are  $L - 2$  unknown entries for  $Y^0$ . Hence, the number of equations is the same as the number of unknowns.

Equation (68) yields  $Z_{n,n+1}^0$ , from which we may obtain  $\kappa^I$  by the use of Eq. (61). If we expand Eq. (56) up to order  $\epsilon$ , we find the relation  $\kappa^I = kS_L/\gamma$  between  $S_L$  and  $\kappa^I$ . Hence,

$$S_L = 2LZ_{n,n+1}^0. \quad (69)$$

Note that, because of Eq. (54),  $Z_{n,n+1}^0$  is independent of  $n$ , even though it depends on  $L$ . The dependence of  $S_L$  on  $L$  is obtained by numerically solving Eq. (68) for  $Z_{n,n+1}^0$ . The result is shown in Fig. 5. As can be seen, it monotonically approaches the value 1. In fact, from our numerical results,  $S_L - 1 \sim (\ln L)/L$  when  $L \rightarrow \infty$ .

We now analyze the next term in the series expansion in order to obtain  $\kappa^{II}$  in Eq. (61). The terms of order  $\epsilon$  in Eqs. (50)–(52) give rise to the following system of equations:

$$(\Gamma'Y^I + Y^I\Gamma') + 2(Y^{II} - \bar{Y}^{II}) = -\nu(A'Z^0 - Z^0A'), \quad (70)$$

$$\nu(A'X^I - X^IA') - 2Z^I = (Z^0\Gamma' + \Gamma'Z^0), \quad (71)$$

$$\nu(A'X^I + X^IA') - 2Y^I = -(Z^0\Gamma' - \Gamma'Z^0). \quad (72)$$

From Eq. (70) we conclude (as just mentioned) that  $Y^{II}$  is not diagonal. Moreover, from the first and last diagonal entries of

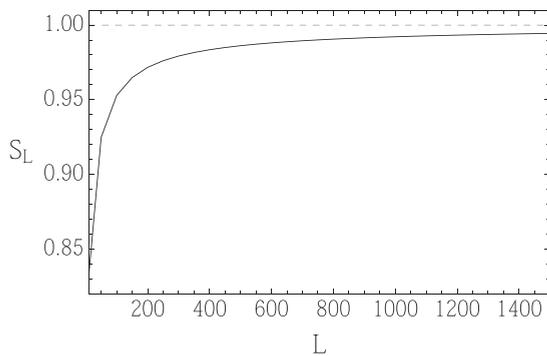


FIG. 5. The function  $S_L = 2LZ_{n,n+1}^0$ , where  $Z^0$  is the solution of Eq. (68).

this equation it follows that

$$Y_{11}^I = -Y_{LL}^I = -\nu Z_{n,n+1}^0, \quad (73)$$

which will again serve as a boundary condition.

Eliminating  $X^I$  in Eqs. (71) and (72), we find that

$$(A'Z^I + Z^IA') = (A'Y^I - Y^IA') - (A'Z^0\Gamma' + \Gamma'Z^0A'). \quad (74)$$

Since the solutions are linear, we may separate  $Y^I$  and  $Z^I$  in two parts as

$$Z^I = Z^I\nu + Z'', \quad (75)$$

$$Y^I = Y^I\nu + Y''. \quad (76)$$

From Eq. (73) we then have that  $Y_{11}^I = -Y_{LL}^I = -Z_{n,n+1}^0$  and  $Y_{11}'' = Y_{LL}'' = 0$ . Separating Eq. (74) in two parts, we find

$$A'Z^I + Z^IA' = A'Y^I - Y^IA', \quad (77)$$

$$A'Z'' + Z''A' = A'Y'' - Y''A' - (A'Z^0\Gamma' + \Gamma'Z^0A'). \quad (78)$$

Now let us analyze our result. Referring back to Eq. (61) for  $\kappa^{II}$ , we may write

$$\kappa^{II} = \frac{2kL}{\gamma}(\nu Z'_{n,n+1} + Z''_{n,n+1}). \quad (79)$$

According to Eq. (77),  $Z'_{n,n+1}$  is given by the same equation as  $Z_{n,n+1}^0$  [Eq. (68)], but with the boundary condition  $Y'_{11} = -Y'_{LL} = -Z_{n,n+1}^0$  instead of  $Y_{11}^0 = -Y_{LL}^0 = 1/2$ . Hence, by linearity

$$Z'_{n,n+1} = -2(Z_{n,n+1}^0)^2. \quad (80)$$

Eq. (60) is, up to order  $1/\lambda^2$ , equivalent to

$$\kappa = \frac{\kappa^I\gamma L}{-\frac{\kappa^{II}}{\kappa^I}\gamma L + \lambda L}, \quad (81)$$

or, which is equivalent,

$$\kappa = \frac{kL(2LZ_{n,n+1}^0)}{\frac{k}{\gamma}(2LZ_{n,n+1}^0) + \gamma(-\frac{LZ''_{n,n+1}}{Z_{n,n+1}^0}) + \lambda L}. \quad (82)$$

By comparing this result with Eq. (56) it is clear that  $S_L = 2LZ_{n,n+1}^0$  and

$$C_L = -\frac{LZ''_{n,n+1}}{Z_{n,n+1}^0}. \quad (83)$$

The dependence of  $C_L$  on  $L$  is obtained by numerically solving Eq. (78), using  $Z^0$ , previously obtained, as input. In Fig. 6 we show the result for  $C_L/S_L$  since it converges much faster with  $L$ . The asymptotic value  $C_\infty = c$  is found to be

$$c = 1.20938909(5). \quad (84)$$

To summarize the results of this section, we have shown that, for large values of  $\lambda$ , the heat conductivity behaves

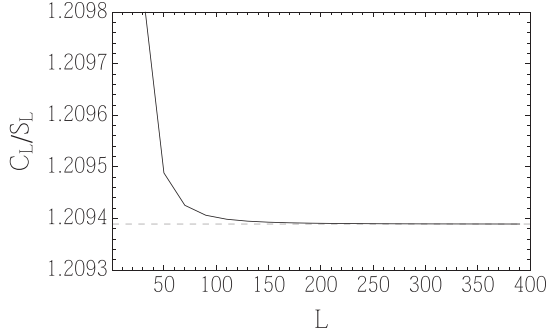


FIG. 6. The ratio  $C_L/S_L$ , where  $C_L$  is given by Eq. (83) and  $Z''$  is the solution of Eq. (78).  $S_L$  is shown in Fig. 5.

according to (56), which for sufficiently large  $L$  reduces to the expression (55) or, which is equivalent, Eq. (4).

### C. Fourier method of computing $S_L$

We now illustrate how to obtain the function  $S_L$  analytically by a different approach. Our goal is again to solve Eq. (68) with  $Y_{11}^0 = -Y_{LL}^0 = 1/2$ . The solution will be based on the assumption that, for large  $L$ , the diagonal matrix  $Y^0$  approaches a linear profile between  $1/2$  and  $-1/2$ . This fact can be verified from the numerical solution of Eq. (68), as illustrated in Fig. 7, which shows the difference  $\Delta Y_{nn}^0$  between the exact numerical solution and the linear interpolation. As can be seen in Fig. 7, this difference vanishes in the limit  $L \rightarrow \infty$ . This assumption is also reasonable given that the diagonal entries of  $Y$  represent the mean-squared velocity profile, which should be linear if the system is to obey Fourier's law. Hence, we shall take

$$Y_{nn}^0 = h(L + 1 - 2n), \quad (85)$$

where  $h = 1/[2(L - 1)]$ , which interpolates linearly between the values  $Y_{11}^0 = 1/2$  and  $Y_{LL}^0 = -1/2$ .

Equation (68) can be solved for  $Z^0$  by diagonalizing  $A$ . The matrix that diagonalizes  $A$  is obtained from its eigenvectors, which are

$$\psi_{kn} = \sqrt{\frac{2}{L+1}} \sin kn, \quad (86)$$

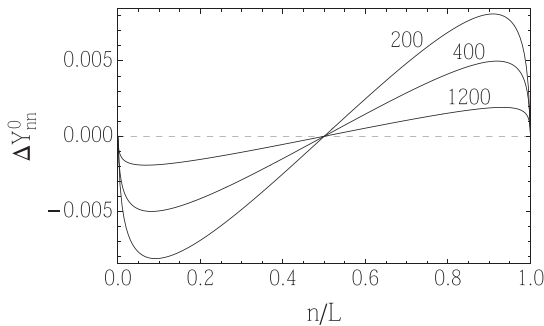


FIG. 7. Difference between the exact numerical solution for  $Y_{nn}^0$  [Eq. (68)] and the linear profile given by the right-hand side of (85) for different system sizes  $L$ , as indicated.

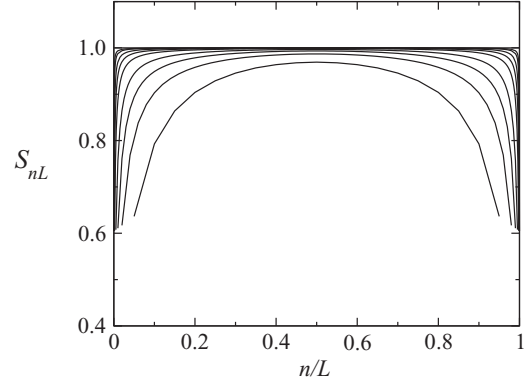


FIG. 8. Numerical calculation of  $S_{nL} = 2LZ_{n,n+1}^0$ , where  $Z_{n,n+1}^0$  is given by Eq. (92). The curves are for different values of  $L$ , from bottom to top, starting at  $L = 20$  and going up to  $L = 10000$ .

where  $k = \pi j/(L + 1)$ ,  $j = 1, 2, \dots, L$ . Defining  $\hat{Y}_{kq}^0$  and  $\hat{Z}_{kq}^0$  by

$$\hat{Y}_{kq}^0 = \sum_{nm} \psi_{kn} Y_{nm}^0 \psi_{qn}, \quad (87)$$

$$\hat{Z}_{kq}^0 = \sum_{nm} \psi_{kn} Z_{nm}^0 \psi_{qn}, \quad (88)$$

where  $q = \pi \ell/(L + 1)$ ,  $\ell = 1, 2, \dots, L$ , we get from Eq. (68) the following relation between these quantities:

$$\hat{Z}_{kq}^0 = \frac{\cos q - \cos k}{2 - \cos k - \cos q} \hat{Y}_{kq}^0. \quad (89)$$

Now, placing (85) into (87) and performing the summation, we get

$$\hat{Y}_{kq}^0 = \frac{-4h \sin k \sin q}{(L+1)(\cos k - \cos q)^2}, \quad (90)$$

valid for odd  $j + \ell$ . When  $j + \ell$  is even, the summation vanishes, and  $\hat{Y}_{kq}^0 = 0$ .

To get  $Z_{nm}^0$  from  $\hat{Z}_{kq}^0$ , we use the inverse transformation,

$$Z_{nm}^0 = \sum_{kq} \psi_{kn} \hat{Z}_{kq}^0 \psi_{qm}. \quad (91)$$

Inserting (90) and (89) into (91) gives

$$Z_{nm}^0 = \frac{8h}{(L+1)^2} \sum_{kq} \frac{\sin kn \sin qm}{2 - \cos k - \cos q} \frac{\sin k \sin q}{\cos k - \cos q}, \quad (92)$$

where the summation is over odd  $j + \ell$ . This sum may be computed numerically for large enough  $L$  and  $m = n + 1$ .

The function  $S_{nL} = 2LZ_{n,n+1}^0$ , computed numerically from Eq. (92), is shown in Fig. 8 for several values of  $L$ . As can be seen, the results depend on  $n$ , a consequence of the linear interpolation approximation (85). However, when  $L \rightarrow \infty$ ,  $S_{nL}$  approach a constant value, namely, the value 1, as seen in Fig. 8, further corroborating the results of Fig. 5 for  $S_L$  when  $L \rightarrow \infty$ , which was precisely the purpose of this calculation.

## V. DISCUSSIONS AND CONCLUSIONS

As our last topic, let us briefly discuss the form of the probability distribution in the NESS. In Appendix B

we show that in the steady state the general solution of the Fokker-Planck equation (7) for  $P(x, v, y, u)$  is, for the potential  $U_1$  in Eq. (12), given by a multivariate Gaussian distribution. This is true only for the potential  $U_1$  and is related to the symmetries of this potential, which imply  $\Theta_1 = \Theta_2$  and  $\Theta_3 = 0$  [see Eqs. (37)–(39)]. Hence, the equilibrium probability distribution when the potential is  $U_1$  is

$$P \sim e^{-\frac{1}{2}x'^t \Theta_1^{-1} x'} e^{-\frac{1}{2}y'^t \Theta_1^{-1} y'}, \quad (93)$$

where  $x' = (x, v)$  and  $y' = (y, u)$ . Since the distribution factors into two parts, we find that the variables in the  $x$  and  $y$  directions are statistically independent.

In conclusion, we have introduced a modification of the harmonic chain whereby all particles are also subject to elastic collisions that conserve the kinetic energy. As was shown, it reproduces Fourier's law irrespective of the intensity of the collisions. These results corroborates our argument that the fine details of the noise are unimportant in leading to Fourier's law; rather, what is relevant is its energy-conserving nature. The model was solved using a numerically exact procedure which is extremely efficient computationally and is valid for any type of harmonic interaction potential. For a particular choice of the interaction potential, we have determined the heat conductivity exactly for small chains and also by an expansion in  $\lambda^{-1}$ . The first term in the expansion was also determined by an approximation that becomes exact in the thermodynamic limit, providing the exact expression

$$\kappa = \frac{k}{\lambda} \quad (94)$$

[see Eq. (55)].

We note that it would be of interest to extend the analysis of the present paper to include anharmonic terms. This, however, is not trivial. The method employed here, which is based on solving directly for the covariances, applies only to harmonic potentials. If that is not the case, then one must resort to the numerical solution of the Langevin equations. This approach is being considered for future publication.

Throughout this paper we have used unit mass and unit lattice spacing. To amend this we simply replace  $k$  by  $k/m$ , where  $m$  is the mass of each particle, and multiply  $\kappa$  by the lattice spacing  $a$ . Reinserting the Boltzmann constant  $k_B$  we find that Eq. (94) becomes

$$\kappa = k_B \frac{ka}{m\lambda}.$$

This equation can also be written in terms of the Young's modulus  $Y = ka$  and the collision characteristic time  $\tau = 1/\lambda$ :

$$\kappa = k_B \frac{Y\tau}{m}. \quad (95)$$

In this form it is identical to  $\kappa = \frac{1}{3}c_v c^2 \tau$  [36], the heat conductivity of solids, where  $c_v$  is the heat capacity per unit volume and  $c$  is the sound velocity. To connect the two equations we recall that  $c_v = 3Nk_B/V = 3k_B\rho/m$ , where  $\rho$  is the density, and also that  $c^2 = Y/\rho$ .

## ACKNOWLEDGMENT

We acknowledge the Brazilian agencies FAPESP and CNPq for financial support.

## APPENDIX A: EXACT SOLUTION FOR SMALL SYSTEMS

Closed forms for the heat conductivity of small chains can be determined by solving the equations for the covariances. This was accomplished using symbolic computing to solve Eq. (35), which is valid specifically for the potential  $U_1$  in Eq. (12). We were able to find the solutions up to  $L = 14$ , in which case there were more than 300 coupled linear equations (hence the need for symbolic computing). The results always have the form of a ratio of polynomials in  $\lambda$ , viz.,

$$\kappa_L = \frac{\sum_{j=0}^M p_j \lambda^j}{\sum_{j=0}^{M+1} q_j \lambda^j}. \quad (A1)$$

The degree of the polynomial in the numerator is  $M$ , and that of the denominator is  $M + 1$ , where  $M$  turns out to be

$$M = \begin{cases} \frac{L^2}{2} - L & \text{if } L \text{ is even,} \\ \frac{L^2}{2} - L + \frac{1}{2} & \text{if } L \text{ is odd.} \end{cases} \quad (A2)$$

For the purpose of illustration, we show the results from  $L = 2$  to  $L = 4$ :

$$\kappa_2 = \frac{2k}{\frac{k}{\gamma} + 2\gamma + 2\lambda},$$

$$\kappa_3 = \frac{3k(k + 2\gamma^2 + 6\gamma\lambda + 4\lambda^2)}{\left(\frac{k^2}{\gamma} + 4k\gamma + 3\gamma^3\right) + (10k + 16\gamma^2)\lambda + \left(4\frac{k}{\gamma} + 27\gamma\right)\lambda^2 + 14\lambda^3},$$

$$\kappa_4 = \frac{4k[(k^2 + 4k\gamma^2 + 3\gamma^4) + (14k\gamma + 22\gamma^3)\lambda + (12k + 59\gamma^2)\lambda^2 + 68\gamma\lambda^3 + 28\lambda^4]}{q_0 + 4(5k^2 + 17k\gamma^2 + 11\gamma^4)\lambda + (12\frac{k^2}{\gamma} + 155k\gamma + 186\gamma^3)\lambda^2 + 6(22k + 63\gamma^2)\lambda^3 + 4(7\frac{k}{\gamma} + 92\gamma)\lambda^4 + 136\lambda^5},$$

where  $q_0 = \left(\frac{k^3}{\gamma} + 6k^2\gamma + 10k\gamma^3 + 4\gamma^5\right)$ .

Retaining the dominant terms in  $\lambda$  in the numerator and denominator, we may cast them in the form (56). This is tantamount to determining exactly the functions  $S_L$  and  $C_L$  in Eq. (56) for small values of  $L$ . The results for  $L = 3$  and  $L = 4$  are  $[\kappa_2$  is

already in the form (56)]

$$\kappa_3 = \frac{\frac{6}{7}(3k)}{\frac{6}{7}\frac{k}{\gamma} + \frac{9}{7}\gamma + 3\lambda}, \quad \kappa_4 = \frac{\frac{14}{17}(4k)}{\frac{14}{17}\frac{k}{\gamma} + \frac{132}{119}\gamma + 4\lambda}, \quad \kappa_5 = \frac{\frac{22}{27}(5k)}{\frac{22}{27}\frac{k}{\gamma} + \frac{311}{297}\gamma + 5\lambda}, \quad \kappa_6 = \frac{\frac{1485}{1823}(6k)}{\frac{1485}{1823}\frac{k}{\gamma} + \frac{307618}{300795}\gamma + 6\lambda}.$$

## APPENDIX B: CONDITIONS FOR THE STATIONARY STATE TO BE GAUSSIAN

In this Appendix we discuss in detail the conditions for the steady state to be described by a Gaussian distribution. Starting from the Fokker-Planck equation (7), we can write down the corresponding equation for the time evolution of the characteristic function,

$$G = \int e^{i(k \cdot x + s \cdot v + q \cdot y + r \cdot u)} P dx dv dy du. \quad (\text{B1})$$

It is more convenient, however, to write down the evolution equation for  $H = \ln G$ , which is

$$\begin{aligned} \frac{\partial H}{\partial t} = \sum_i \left\{ k_i \frac{\partial H}{\partial s_i} + q_i \frac{\partial H}{\partial r_i} - s_i \sum_j \left( A_{ij} \frac{\partial H}{\partial k_j} + C_{ij} \frac{\partial H}{\partial q_j} \right) - r_i \sum_j \left( B_{ij} \frac{\partial H}{\partial q_j} + C_{ij} \frac{\partial H}{\partial k_j} \right) - (\gamma_i + \lambda) \left( s_i \frac{\partial H}{\partial s_i} + r_i \frac{\partial H}{\partial r_i} \right) \right. \\ \left. - \gamma_i T_i (s_i^2 + r_i^2) + \lambda \left( s_i^2 \frac{\partial^2 H}{\partial r_i^2} + r_i^2 \frac{\partial^2 H}{\partial s_i^2} - 2s_i r_i \frac{\partial^2 H}{\partial s_i \partial r_i} \right) + \lambda \left( s_i \frac{\partial H}{\partial r_i} - r_i \frac{\partial H}{\partial s_i} \right)^2 \right\}, \quad (\text{B2}) \end{aligned}$$

where  $A$ ,  $B$ , and  $C$  are the matrix elements of the potential appearing in Eq. (11). It is known that if  $H$  is a quadratic form on the variables  $k_i$ ,  $s_i$ ,  $q_i$ , and  $r_i$  (which means  $G$  is Gaussian), then the probability distribution will be Gaussian. We will show that this is indeed the case when the potential is  $U_1$ , Eq. (12), which is the form we focused on throughout the paper [see Eqs. (37)–(39)].

To investigate the steady state we set  $\partial H / \partial t = 0$ . We start by assuming that  $H$  is a quadratic form in the variables  $k_i$ ,  $s_i$ ,  $q_i$ , and  $r_i$ , with unknown coefficients, which turn out to be precisely the entries of the covariance matrix  $\Theta$  in Eq. (24). This form is then inserted in Eq. (B2) and equated to zero. All terms on the right-hand side produce quadratic forms, except the very last one. Thus, if this term is absent, the quadratic form will be a solution, and the probability distribution will be Gaussian.

Let us consider this last term explicitly. It suffices to consider only the part corresponding to the  $i$ th particle, which we write for simplicity as  $H_i$ . We take it to be a quadratic function in  $s_i$  and  $r_i$  (the terms proportional to  $k_i$  and  $q_i$  are unimportant for the argument):

$$H_i = \theta_1 s_i^2 + \theta_2 r_i^2 + \theta_3 s_i r_i. \quad (\text{B3})$$

Note that  $\theta_1$ ,  $\theta_2$ , and  $\theta_3$  are entries of the covariance matrices  $\Theta_1$ ,  $\Theta_2$ , and  $\Theta_3$  in Eq. (24), respectively. The last term in Eq. (B2) then becomes

$$\left[ s_i \frac{\partial H_i}{\partial r_i} - r_i \frac{\partial H_i}{\partial s_i} \right]^2 = [2s_i r_i (\theta_2 - \theta_1) + \theta_3 (s_i^2 - r_i^2)]^2. \quad (\text{B4})$$

We thus reach the conclusion that for this last term to vanish, we must have  $\theta_2 = \theta_1$  ( $x$  and  $y$  velocity covariances should be symmetrical) and  $\theta_3 = 0$  (velocity cross-covariances should be null). This is precisely the case for the potential  $U_1$  in Eq. (12), for which  $\Theta_1 = \Theta_2$  and  $\Theta_3 = 0$ , as shown in Eqs. (37)–(39). We therefore conclude that, for the potential  $U_1$ , a Gaussian form is a valid solution for the characteristic function:

$$G = e^{-\frac{1}{2} k'^t \Theta_1 k'} e^{-\frac{1}{2} q'^t \Theta_1 q'}, \quad (\text{B5})$$

where  $k' = (k, s)$  and  $q' = (q, r)$ . Taking the inverse transform, we then arrive at the Gaussian form in Eq. (93) for the steady-state distribution  $P$ .

- 
- |  |   |
|--|---|
| <p>[1] Z. Rieder, J. L. Lebowitz, and E. Lieb, <i>J. Math. Phys.</i> <b>8</b>, 1073 (1967).</p> <p>[2] S. Lepri, R. Livi, and A. Politi, <i>Phys. Rev. Lett.</i> <b>78</b>, 1896 (1997).</p> <p>[3] K. Aoki and D. Kusnezov, <i>Phys. Rev. Lett.</i> <b>86</b>, 4029 (2001).</p> <p>[4] J.-P. Eckmann and L.-S. Young, <i>Europhys. Lett.</i> <b>68</b>, 790 (2004).</p> <p>[5] P. Cipriani, S. Denisov, and A. Politi, <i>Phys. Rev. Lett.</i> <b>94</b>, 244301 (2005).</p> <p>[6] E. Pereira and R. Falcão, <i>Phys. Rev. Lett.</i> <b>96</b>, 100601 (2006).</p> <p>[7] T. Mai, A. Dhar, and O. Narayan, <i>Phys. Rev. Lett.</i> <b>98</b>, 184301 (2007).</p> | <p>[8] J. Lukkarinen and H. Spohn, <i>Commun. Pure Appl. Math.</i> <b>61</b>, 1753 (2008).</p> <p>[9] A. Gerschenfeld, B. Derrida, and J. L. Lebowitz, <i>J. Stat. Phys.</i> <b>141</b>, 757 (2010).</p> <p>[10] C. Bernardin and S. Olla, <i>J. Stat. Phys.</i> <b>145</b>, 1244 (2011).</p> <p>[11] D. Roy, <i>Phys. Rev. E</i> <b>86</b>, 041102 (2012).</p> <p>[12] H. van Beijeren, <i>Phys. Rev. Lett.</i> <b>108</b>, 180601 (2012).</p> <p>[13] A. Dhar, <i>Phys. Rev. Lett.</i> <b>86</b>, 3554 (2001).</p> <p>[14] E. Pereira and H. C. F. Lemos, <i>Phys. Rev. E</i> <b>78</b>, 031108 (2008).</p> |
|--|---|

- [15] M. Bolsterli, M. Rich, and W. M. Visscher, *Phys. Rev. A* **1**, 1086 (1970).
- [16] F. Bonetto, J. L. Lebowitz, and J. Lukkarinen, *J. Stat. Phys.* **116**, 783 (2004).
- [17] E. Pereira and R. Falcão, *Phys. Rev. E* **70**, 046105 (2004).
- [18] L. Delfini, S. Lepri, R. Livi, and A. Politi, *Phys. Rev. E* **73**, 060201 (2006).
- [19] O. Narayan and S. Ramaswamy, *Phys. Rev. Lett.* **89**, 200601 (2002).
- [20] P. Grassberger, W. Nadler, and L. Yang, *Phys. Rev. Lett.* **89**, 180601 (2002).
- [21] J. M. Deutsch and O. Narayan, *Phys. Rev. E* **68**, 010201(R) (2003).
- [22] G. Casati and T. Prosen, *Phys. Rev. E* **67**, 015203(R) (2003).
- [23] G. Basile, C. Bernardin, and S. Olla, *Commun. Math. Phys.* **287**, 67 (2009).
- [24] Y. Dubi and M. Di Ventra, *Phys. Rev. E* **79**, 042101 (2009).
- [25] Y. Dubi and M. Di Ventra, *Phys. Rev. B* **79**, 115415 (2009).
- [26] S. Lepri, C. Mejía-Monasterio, and A. Politi, *J. Phys. A* **42**, 025001 (2009).
- [27] C. Bernardin and S. Olla, *J. Stat. Phys.* **121**, 271 (2005).
- [28] C. Giardinà, J. Kurchan, and F. Redig, *J. Math. Phys.* **48**, 033301 (2007).
- [29] C. Kipnis, C. Marchioro, and E. Presutti, *J. Stat. Phys.* **27**, 65 (1982).
- [30] A. Iacobucci, F. Legoll, S. Olla, and G. Stolz, *J. Stat. Phys.* **140**, 336 (2010).
- [31] S. Lepri, R. Livi, and A. Politi, *Phys. Rep.* **377**, 1 (2003).
- [32] A. Dhar, *Adv. Phys.* **57**, 457 (2008).
- [33] G. T. Landi and M. J. de Oliveira, *Phys. Rev. E* **87**, 052126 (2013).
- [34] A. Dhar, K. Venkateshan, and J. L. Lebowitz, *Phys. Rev. E* **83**, 021108 (2011).
- [35] D. S. Lemons, *An Introduction to Stochastic Processes in Physics* (Johns Hopkins University Press, Baltimore, 2002).
- [36] N. W. Ashcroft and N. D. Mermin, *Solid State Physics* (Brooks/Cole, Fort Worth, 1976), Chap. 25, Eq. (25.31).